Nucleic Acids Research, 1995, Vol. 23, No. 16 3161–3167

Cleavage of tRNA with imidazole and spermine imidazole constructs: a new approach for probing RNA structure

Valentin V. Vlassov[1,2], Guy Zuber[3], Brice Felden[4], Jean-Paul Behr[3] and Richard Giegé[4,*]

[1]Institute of Bioorganic Chemistry, Siberian Division of the Russian Academy of Sciences, 8 Lavrentiev Avenue, Novosibirsk 630090, Russia, [2]Novosibirsk State University, Novosibirsk 630090, Russia, [3]Laboratoire de Chimie Génétique, Université Louis Pasteur, URA 1386 du CNRS, Faculté de Pharmacie, 74 route du Rhin, F-67401 Illkirch Cedex, France and [4]UPR 9002 du CNRS 'Structure des Macromolécules Biologiques et Mécanismes de Reconnaissance', Institut de Biologie Moléculaire et Cellulaire du CNRS, 15 rue René Descartes, F-67084 Strasbourg Cedex, France

Received May 30, 1995; Revised and Accepted July 12, 1995

ABSTRACT

Hydrolysis of RNA in imidazole buffer and by spermine–imidazole conjugates has been investigated. The RNA models were yeast $tRNA^{Asp}$ and a transcript derived from the 3′-terminal sequence of tobacco mosaic virus RNA representing a minihelix capable of being enzymatically aminoacylated with histidine. Imidazole buffer and spermine–imidazole conjugates in the presence of free imidazole cleave phosphodiester bonds in the folded RNAs in a specific fashion. Imidazole buffer induces cleavages preferentially in single-stranded regions because nucleotides in these regions have more conformational freedom and can assume more easily the geometry needed for formation of the hydrolysis intermediate state. Spermine–imidazole constructs supplemented with free imidazole cleave $tRNA^{Asp}$ within single-stranded regions after pyrimidine residues with a marked preference for pyrimidine-A sequences. Hydrolysis patterns suggest a cleavage mechanism involving an attack by the imidazole residue of the electrostatically bound spermine–imidazole and by free imidazole at the most accessible single-stranded regions of the RNA. Cleavages in a viral RNA fragment recapitulating a tRNA-like domain were found in agreement with the model of this molecule that accounts for its functional properties, thus illustrating the potential of the imidazole-derived reagents as structural probes for solution mapping of RNAs. The cleavage reactions are simple to perform, provide information reflecting the state of the ribose–phosphate backbone of RNA and can be used for mapping single- and double-stranded regions in RNAs.

INTRODUCTION

Small RNA cleaving molecules are extensively used as probes for the investigation of RNA structures in solution (e.g. 1–6). The groups capable of catalytically hydrolysing RNA are considered as perspective groups for the design of efficient antisense oligonucleotide derivatives (7–10). In an attempt to develop efficient catalytic RNA cleaving groups, mimics of active centres of RNases have been synthesised and tested (11–13). The sufficiency of imidazole groups to imitate the active centre of RNase (14) (Fig. 1A) has been suggested by the possibility to hydrolyse RNA in concentrated imidazole buffer (15–17).

Recently we have mimicked the active centre of RNase A with small molecules containing two imidazole residues conjugated to an intercalating phenazine dye by linkers of variable length and flexibility (13) (**Phen-Im** in Fig. 1B). In the course of these studies we were led to investigate hydrolysis of RNA by conjugates of spermine and imidazole and by imidazole buffer. Here we describe RNA hydrolysis with imidazole and with spermine–imidazole constructs (Fig. 1B) which act on RNA in the presence of imidazole buffer. The constructs contain a polycationic moiety which binds to the negatively-charged ribose–phosphate backbone and bring the conjugated imidazole residue in close contact with the phosphates and riboses. The second imidazole residue needed for the hydrolysis is provided by the buffer. We tested the specificity of the reagents on an RNA with known structure, $tRNA^{Asp}$ and on a pseudo-knot containing RNA molecule and found that the cleavage patterns produced by imidazole and the imidazole constructs reflect the conformational state of the RNA.

MATERIALS AND METHODS

Chemical reagents and enzymes

Imidazole (buffer grade) from Merck was used without any additional purification. Spermine–imidazole constructs were synthesised as previously described (18). All buffer solutions were prepared from Milli-Q water, contained 1 mM EDTA, and were filtered through membrane filters Millex GS from Millipore with 0.2 μm pores.

Rotiphorese Gel 40 solution of acrylamide and bis-acrylamide was from Carl Roth GmbH (Karlsruhe, Germany). [γ-^{32}P]ATP

* To whom correspondence should be addressed

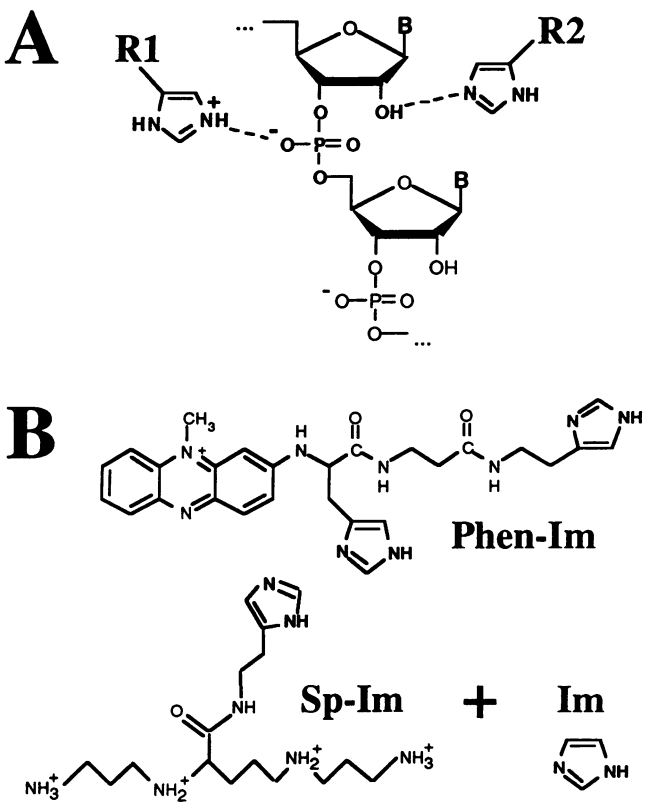

Figure 1. (**A**) Scheme of RNA hydrolysis by RNase A (adapted from refs 14 and 15). Two imidazoles of histidine residues of the enzyme act as acidic and basic imidazolium and imidazole units, respectively (14). At the first step of the process, the ester interchange to form a cyclic phosphate occurs, which results in scission of the RNA chain. Then the formed 2′,3′-cyclic phosphate ester is hydrolysed by the enzyme. (**B**) Structure of the conjugates bearing imidazole residues and groups capable of non-covalent interaction with nucleic acids (**Phen-Im** and **Sp-Im**). Two more spermine imidazole conjugates have been tested, which were similar to **Sp-Im** except that the imidazole residue was methylated at nitrogen 1 (**Sp-Im-1**) and nitrogen 3 (**Sp-Im-3**).

(3000 Ci/mmol), [α-^{32}P]ATP (400 Ci/mmol) and [α-^{32}P]pCp (3000 Ci/mmol) were from Amersham (Les Ulis, France). T4 polynucleotide kinase was from Amersham, snake venom phosphodiesterase from Worthington (Freehold, NJ) and bacterial alkaline phosphatase from Appligène (Strasbourg, France). T7 RNA polymerase was prepared according to (19) and (ATP:CTP) tRNA nucleotidyl-transferase according to (20). *Nsi*I restriction nuclease was from Gibco BRL (Bethesda, ML) and RNasin from Promega (Madison, WI). Enzymes and chemicals used for end-labelling of RNA and electrophoresis were as described in (21). All other products were of the highest quality available.

RNAs

Total yeast tRNA, used as carrier to supplement labelled RNAs, was from Boehringer-Mannheim (Meylan, France). Native yeast tRNA^{Asp} was obtained from total tRNA by established procedures (22). A 38 nucleotide-long RNA, derived from the 3′-terminal sequence of tobacco mosaic virus (TMV, wild strain) (23) and corresponding to a minihelix recapitulating the acceptor branch of the viral tRNA-like domain, was cloned downstream of the T7 RNA polymerase promoter as described earlier (24). Plasmids were linearised by *Nsi*I restriction nuclease before transcription so that transcripts will end with the 3′-terminal CCA triplet. Transcription mixtures contained 40 mM Tris–HCl pH 8.0, 22 mM $MgCl_2$, 1 mM spermidine, 5 mM DTT, 0.01% Triton X100, 40 U RNasin, 4 mM each of the NTP, 15 μg linearised DNA for 50 μl transcription mixture, and 500 U T7 RNA polymerase. After incubation for 3 h at 37°C, reactions were stopped by a 1:1 phenol/ether extraction followed by ethanol precipitation. Transcripts were separated from non-incorporated nucleotides and DNA by gel electrophoresis. Appropriate bands were electroeluted and pure transcripts recovered by ethanol precipitation. Routinely, 10 μg of transcript were obtained from 1 μg of template. RNA concentrations were determined spectrophotometrically, assuming 1 absorbance unit at 260 nm corresponds to 40 μg/ml RNA in a 1 cm path-length cell.

End-labelling of RNAs

5′-end-labelling of RNA with [γ-^{32}P]ATP was done as previously described (21,25). To introduce radiolabel at the 3′-end of the tRNA^{Asp}, the CCA 3′-end of the tRNA was removed by a partial digestion by phosphodiesterase and restored by (ATP:CTP) tRNA nucleotidyl-transferase in the presence of the [α^{32}P]ATP as described (21). Labelling at the 3′-end of the TMV minihelix was performed by ligation of [α-^{32}P]pCp with the T4 RNA ligase according to (27). After labelling, RNAs were purified by electrophoresis in 12% denaturing polyacrylamide gels. The labelled RNAs were eluted from gels by 125 mM ammonium acetate at pH 6.0 containing 0.5 mM EDTA and 0.025% SDS. After ethanol precipitation, RNAs were dissolved in water and stored at –20°C.

Cleavage conditions

Reaction mixtures contained 5′- or 3′-end labelled RNAs (50–100 000 Cerenkov c.p.m.) supplemented by 1 μg of carrier tRNA dissolved in 20 μl of appropriate buffer, as described in the text. After incubation, 20 μl of 0.3 M sodium acetate at pH 5.0 was added to each probe followed by 400 μl of a 2% solution of lithium perchlorate in acetone. The precipitated RNA was recovered by centrifugation and the precipitate was washed with 400 μl of acetone and dried. Samples were dissolved in 7 M urea containing 0.1% bromophenol blue and xylene cyanol and subjected to electrophoresis through a denaturing polyacrylamide gel (12% acrylamide, 7 M urea, 30 × 40 × 0.04 cm^3).

Quantitation of the cleavage patterns

Cleavage patterns were quantitated using a FUJIX Bio-Imaging Analyzer BAS 2000 system. Photostimulatable imaging plates (type BAS-III from Fuji Photo Film Co, Ltd, Japan) were pressed on gels and exposed at room temperature for 30 min. Imaging plates were analysed by performing volume integrations of specific cleavage sites and reference blocks using the FUJIX BAS 2000 Work Station Software (version 1.1).

RESULTS AND DISCUSSION

Basic observations with imidazole

Figure 2 displays a typical autoradiogram of the cleavage pattern by imidazole of 3′-end-labelled tRNA^{Asp}. It is seen that random cleavage of tRNA occurs at high temperature when the molecule

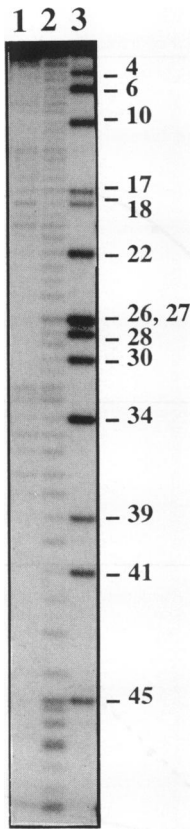

Figure 2. Cleavage of yeast $tRNA^{Asp}$ in imidazole buffer. The figure displays a typical electrophoregram of the cleavage products generated as a result of incubations of the 3′-end labelled tRNA in imidazole buffers in different conditions. Lane 1, $tRNA^{Asp}$ incubated at 37°C for 12 h in 2.0 M imidazole buffer pH 7.0 containing 40 mM NaCl, 10 mM $MgCl_2$ and 1 mM EDTA; lane 2, $tRNA^{Asp}$ incubated for 10 min at 90°C in 2.0 M imidazole buffer, at pH 7.0 containing 0.5 mM EDTA; lane 3, partial RNase T1 digest.

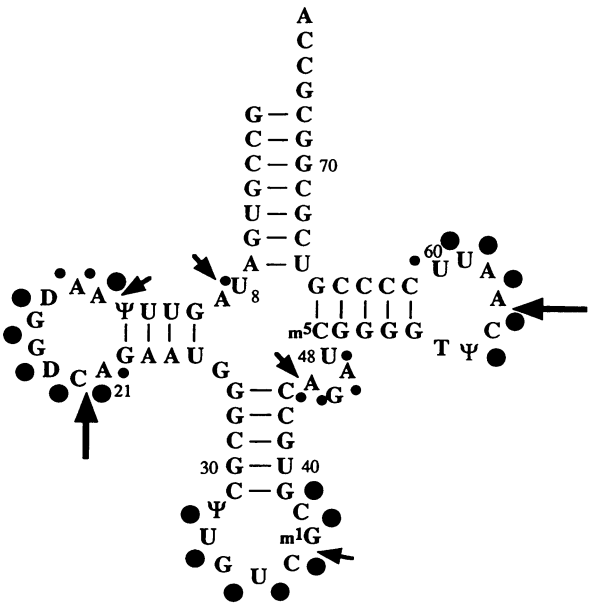

Figure 3. Cloverleaf structure of yeast $tRNA^{Asp}$ (40) with imidazole induced cleavage points. Phosphodiester linkages displaying enhanced susceptibility to hydrolysis by the imidazole buffer in conditions stabilising the RNA structure are indicated by dots with diameters proportional to the intensity of the cuts. Phosphodiester linkages attacked by the **Sp-Im** nuclease in the presence of imidazole buffer are indicated by arrows which lengths are proportional to the intensity of the cuts.

is unfolded (lane 2) and that the cleavage occurs essentially non-randomly when the reaction is performed in conditions stabilising the RNA structure, i.e. at low temperature and in the presence of magnesium ions (lane 1). The location of the cleavages within the $tRNA^{Asp}$ sequence is shown in Figure 3.

The dependence of the cleavage reaction on experimental conditions is shown in Figure 4. Yield of hydrolysis increases with the increase of imidazole concentration and significant cuts are generated for imidazole concentrations above 1 M (Fig. 4a). In accordance with earlier reports (16), the hydrolysis rate increases with the first power of the buffer concentration. This linear dependence may be explained by increased concentration of the protonated form of imidazole in the vicinity of the polyanionic RNA. Due to this, the protonated imidazole is always present in excess and reaction should be dependent linearly on the concentration of the second required species, non-protonated imidazole. The effects of pH and incubation times on $tRNA^{Asp}$ hydrolysis are illustrated in Figure 4b and c. As expected, intensity of cleavage increases with incubation time and pH optimum of the reaction is pH ~7.0. This behaviour is consistent with the imidazole promoted hydrolytic mechanisms, similar to that of RNase A, involving imidazole moieties in equimolar equilibrium between deprotonated imidazole and protonated imidazolium forms (14–17). Increasing temperature results in enhancement of reactivity of phosphodiester bonds protected from hydrolysis by the RNA structure (Fig. 4d). In controls where imidazole was replaced by a HEPES buffer at pH 7.0, spontaneous degradation of tRNA was negligible. Finally, it was found that 1-methylimidazole buffer also catalyses hydrolysis of RNA, although with an efficiency 3- to 4-fold lower, as compared with that of imidazole (data not shown).

The above data correspond to average cleavage extents for a large number of phosphodiester bonds scattered over the structure of tRNA. Therefore it is not excluded that slight mechanistic differences exist for the cleavage of individual bonds linked to different structural environments in the tRNA or, as discussed for the hydrolysis of model compounds (28), to special medium conditions around these bonds. Also it is clear that for incubations at high pH, the acid/base cleavage mechanism mimicking the action of RNase A is accompanied by an hydroxy de-catalysed reaction.

Specificity and mechanism of cleavage of RNA in imidazole buffer

As seen in Figure 2, cleavages occur predominantly within the single-stranded regions of the $tRNA^{Asp}$ cloverleaf (Fig. 3). Phosphodiester bonds in the double-stranded regions of the molecule are more resistant to imidazole hydrolysis. Resistance to hydrolysis appears also at the 5′-sides of the anticodon loop and the T-loop. These observations demonstrate the potential of imidazole buffer to cleave RNA in a specific way reflecting features of the secondary structure of the molecule. The decreased rate of the cleavage within the double-stranded regions of RNA

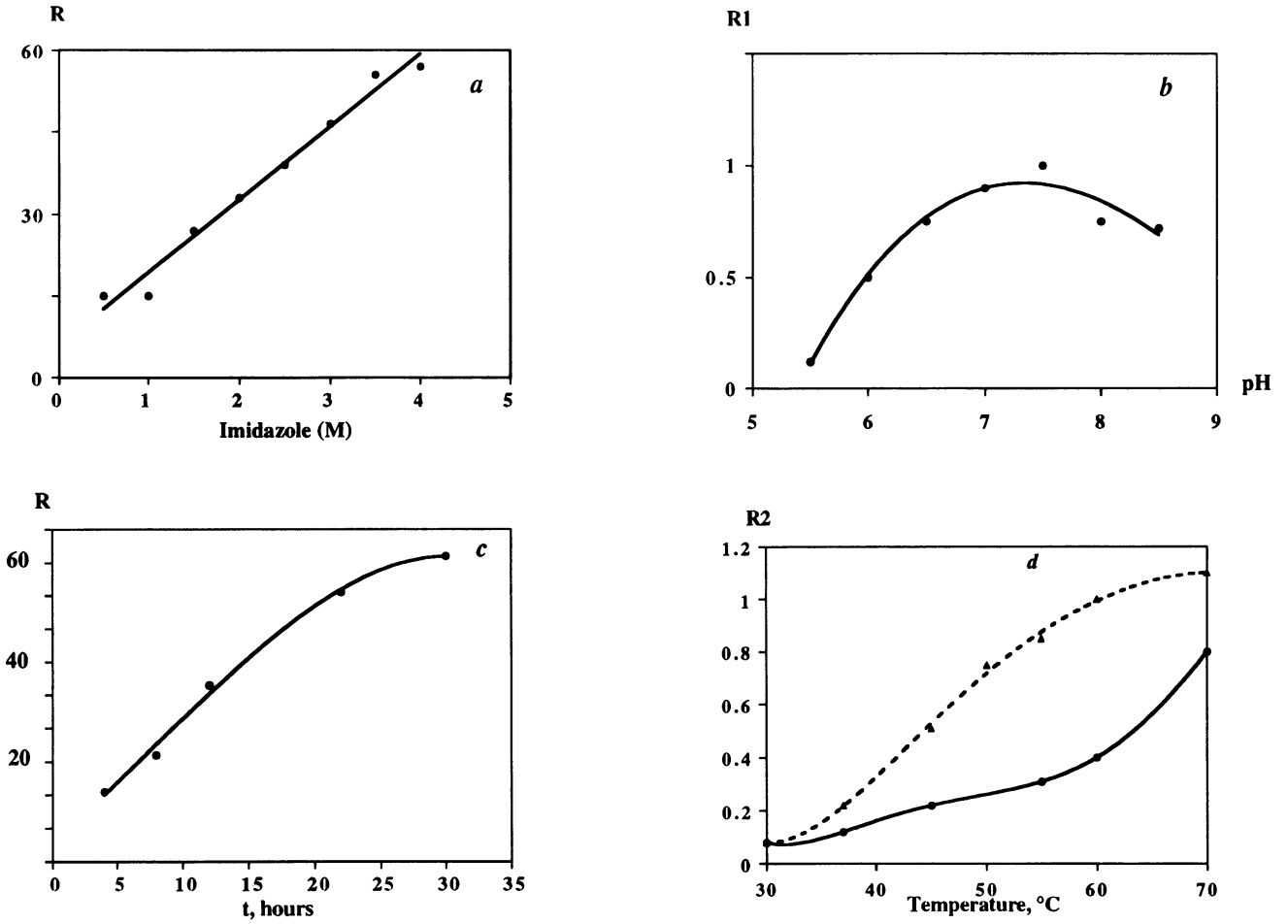

Figure 4. Effect of experimental conditions on the imidazole induced cleavage extent of yeast $tRNA^{Asp}$. All experiments were performed at 37°C. (**a**) Effect of imidazole concentration. R, extent of RNA hydrolysis (summation of all cleavage products), in percents of the total amount of radioactive RNA deposited on the gels. Reaction mixtures were incubated for 12 h in imidazole buffer at pH 7.0. (**b**) Effect of pH on the tRNA hydrolysis in 2.0 M imidazole buffer at 37°C, incubation time 12 h. **R1**, relative hydrolysis extent: ratio of the hydrolysis extent at a given pH to that achieved at pH 7.0. (**c**) Effect of incubation time on hydrolysis of the tRNA in 2.0 M imidazole buffer at pH 7.0. **R**, extent of the tRNA cleavage, in per cents. (**d**) Hydrolysis of phosphodiester bonds in the T-stem (dots, groups of phosphodiester bonds 49–54 and 60–64) and in the anticodon stem (triangles, groups of phosphodiester bonds 26–31 and 39–42) of $tRNA^{Asp}$ in imidazole buffer at different temperatures. The tRNA was incubated in 2.0 M imidazole buffer, pH 7.0 containing 40 mM NaCl, 1 mM EDTA and 10 mM $MgCl_2$ for 25 h at 30°C, 12 h at 37°C, 8 h at 45°C, 5 h at 50°C, 3.5 h at 55°C, 2 h at 60°C and 1 h at 70°C. The incubation times at different temperatures have been selected so as to provide similar extent of cleavage of the exposed phosphodiester bonds in the anticodon loop of the molecule. **R2**, relative cleavage extent at the group of phosphodiester bonds determined as ratio of intensity of the group of bands corresponding to cleavages at given phosphodiester bonds to the group of bands corresponding to the cleavage at the phosphodiester bonds in the anticodon loop (phosphodiester bonds 32–38).

and at the 5′-side of the loops where nucleotides are in a stacked conformation (29) can be explained by the increased rigidity of the RNA backbone in these regions. This rigidity interferes with conformational changes needed for the appropriate orientation of the phosphodiester bond and the sugar for the trans-esterification step of the reaction. A similar explanation holds for the spontaneous cleavages of hydrolytic nature of RNAs, including $tRNA^{Asp}$, that also occur predominantly in single-stranded regions (e.g. 21,30,31).

By analogy with the enzymatic mechanism demonstrated for RNase A (14,15), a cleavage event catalysed by the imidazole reagents on tRNA, results in the formation of a fragment having a 5′-hydroxyl and a second fragment having a 3′-phosphate group. This conclusion is consistent with the electrophoretic mobility of the degradation products that migrate like oligonucleotides generated by RNase T1 or by alkaline hydrolysis (see Fig. 2).

It should be noted that hydrolysis in imidazole buffer at high temperature provides a simple method for producing RNA ladders at neutral pH, which is an advantage for RNAs containing alkali-sensitive bases. The latters are partially destroyed in the traditional hydrolysis conditions which results in doubling of electrophoretic bands and strongly enhanced bands at the positions corresponding to the pH-sensitive nucleotides. This is, for example, the case for the m^7G containing tRNAs (31).

Cleavage with spermine–imidazole conjugates

We expected that due to electrostatic interaction, the spermine–imidazole constructs (Fig. 1B) would bind to RNA and bring the

conjugated imidazole residue in contact with the phosphodiester backbone of the RNA. The second imidazole needed for the reaction would be provided as a free molecule by the imidazole buffer. It was found that the constructs indeed cleave tRNA in the presence of imidazole.

Figure 5 displays a typical autoradiogram of the cleavage patterns of 3′-end-labelled $tRNA^{Asp}$ by the spermine–imidazole conjugates (**Sp-Im**, **Sp-Im-1** and **Sp-Im-3**). The derivatives generate a non-random hydrolysis pattern with two major and several faint bands. Cleavage positions are similar to those observed for the conjugate **Phen-Im** (13), although relative intensities of cuts are different. The intensity of cleavage is highest with **Sp-Im**, in accordance with the above-mentioned observations on higher hydrolysing efficiency of imidazole as compared to the *N*-methylated imidazole. This is further evidence that it is the imidazole residue of the conjugate which catalyses hydrolysis. Spontaneous degradation of tRNA under these conditions, either in the absence of the reagents, in the presence of **Sp-Im** without imidazole buffer, or in 50 mM imidazole buffer in the absence of the constructs is negligible. The fact, that the constructs and diluted imidazole buffer alone are inactive is also strong evidence that hydrolysis is not caused by contaminants, like traces of RNases or metal ions. The tRNA cleavage by **Sp-Im** is stimulated optimally at concentrations of the imidazole buffer in the 50–100 mM range. Further increase of buffer concentration inhibits the reaction, likely because of the displacement of **Sp-Im** from RNA due to the increased ionic strength of the solution. Incubation of RNA with **Sp-Im** for 48 h in optimal reaction conditions results in complete hydrolysis of the tRNA, as evidenced by disappearance on the gels of the tRNA band accompanied by a decrease of the intensity of bands of longest oligonucleotides and a concomitant increase of those of shortest oligonucleotides. Sufficiency of low concentrations of imidazole buffer for the hydrolysis in the presence of the conjugates can be explained by electrostatic effects. Thus, the buffer supplies the protonated imidazole species, which is present at increased concentration in the vicinity of the polyanionic tRNA and the main role of the conjugate consists of providing high local concentration of the non-protonated imidazole.

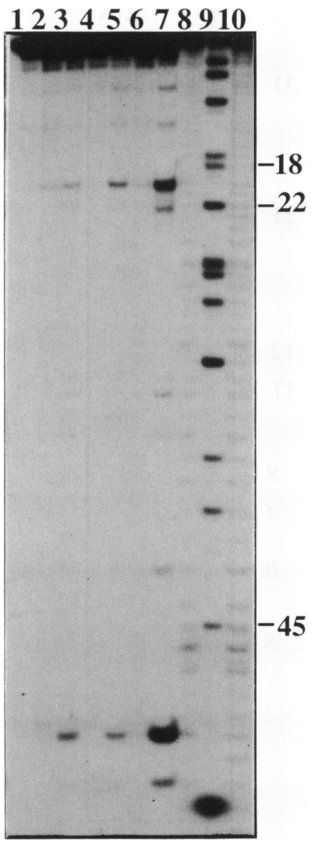

Figure 5. Cleavage of $tRNA^{Asp}$ by histamine conjugates in 40 mM HEPES buffer at pH 7.0 (lanes 2, 4 and 6) or in 50 mM imidazole buffer at pH 7.0 (lanes 3, 5 and 7). The figure displays an electrophoregram of the RNA cleavage pattern. Lane 1, control incubation of the tRNA in 50 mM imidazole buffer at pH 7.0; lanes 2 and 3, tRNA incubated with 2.5 mM **Sp-Im-1**; lanes 4 and 5, tRNA incubated with 2.5 mM **Sp-Im-3**; lanes 6 and 7, tRNA incubated with 2.5 mM **Sp-Im**; lane 8, partial alkaline cleavage of the tRNA; lane 9, partial RNase T1 digest of the tRNA; lane 10, tRNA incubated for 10 min at 90°C in 2.0 M imidazole buffer at pH 7.0 containing 0.5 mM EDTA.

Specificity of the spermine–imidazole promoted cleavages

The major cleavages by spermine–imidazole conjugates occur at two CpA sequences at positions 55–56 and 20–21 in $tRNA^{Asp}$ (Figs 3 and 5). Less intense cuts are observed after U8, Ψ13, C36 and C43. All cleavages occur after pyrimidine residues and for the most intense they are within 5′-PypA-3′ sequences, in particular CpA. The cleavage pattern of the tRNA can be affected by two factors: the reactivities of individual phosphodiester bonds and the specificity of binding of the cationic molecules at the tRNA surface. This pattern is in agreement with the known spermine binding sites in $tRNA^{Asp}$ identified by affinity modification with a photoreactive spermine conjugate (3). One of the spermine binding sites is in the vicinity of phosphates 9–11, another between phosphates 23–26 and 41–44, and one or two additional sites are in a cleft formed between juxtaposed phosphates of the D- and T-loops. The minor cut at phosphodiester bond 8, likely originates from the **Sp-Im** bound in the first site and the other cut at position 43 corresponds to the second spermine binding site. The strongest cuts at positions 20 and 56 are produced by the reagents bound between the T- and D-loops. These are the sites where the bound photoreactive spermine conjugates modify nucleosides in positions 20–25 and 57–61 (3). Another minor cut by **Sp-Im** at phosphodiester bond 36 occurs also in agreement with the data on interaction of the photoreactive spermine conjugate with nucleosides 33–34 (3). The $tRNA^{Asp}$ cleavage pattern by **Sp-Im** is similar but not identical to that produced by the **Phen-Im** constructs containing two imidazole residues attached to an intercalating dye (13). In the latter case the major cleaving site at position 56 is one order of magnitude more intensive than cleavages at any other sites, while the **Sp-Im** constructs show marked preference to phosphodiester bonds at position 20 and 56. Likely these reactivity differences are due to differences in the binding mode of the cleaving molecules at the tRNA surface. Thus, specificity is mainly governed by the reactivity of individual phosphodiester bonds, modulated by the binding pattern of the cleaving molecules on the tRNA structure.

Cleavage specificity of the spermine–imidazole constructs is different from that observed for tRNA hydrolysis by concentrated imidazole buffer. In such a buffer, all phosphodiester bonds in single-stranded regions are hydrolysed at similar rates. A source of the difference may be that small free imidazole molecules can

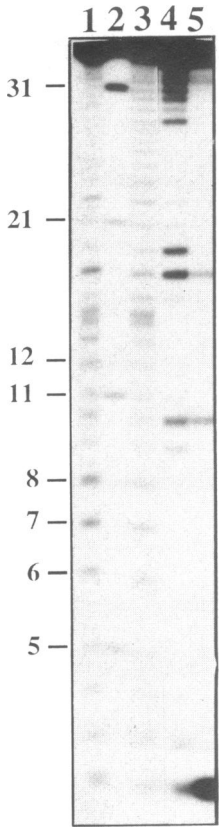

Figure 6. Cleavage of the RNA transcript derived from the TMV tRNA-like domain (23) in imidazole buffer. Lane 1, partial alkaline hydrolysis; lane 2, partial RNase T1 hydrolysis; lane 3, incubation for 10 min at 90°C in 2.0 M imidazole buffer at pH 7.0; lane 4, incubation for 16 h at 25°C in 2.0 M imidazole buffer at pH 7.0 containing 40 mM NaCl, 1 mM EDTA and 10 mM $MgCl_2$; lane 5, hydrolysis by a binary chemical nuclease consisting of 2 mM **Sp-Im** and 50 mM imidazole at pH 7.0, with an incubation of 7 h at 37°C.

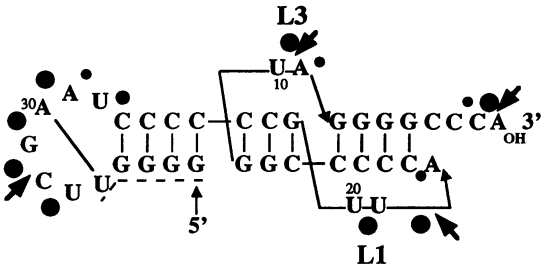

Figure 7. Secondary structure of the RNA transcript derived from the TMV tRNA-like domain with imidazole induced cleavage points indicated by dots at the residues after which cleavage occurs. Diameters of the dots are proportional to the intensity of the cuts. Arrows indicate the residues after which phosphodiester bonds are attacked by the binary chemical nuclease. L1 and L3 emphasise the two single-strands of the pseudo-knot crossing the deep and the shallow grooves, respectively (see ref. 41 for details on pseudo-knots). The dashed line indicates the nucleotides which could not be tested for methodological reasons.

reach riboses and phosphates of RNA easily from different directions without disturbing the RNA structure. In the case of the conjugates and RNase, the cleaving molecules bind to RNA and thus can affect, to different extents, conformation, flexibility and accessibility of phosphodiester bonds in different dinucleotide sequences. Apparently, a favourable situation is realised for PypPu sequences. The instability of such sequences in RNA is a known phenomenon (21,30,31,33–35) the mechanism of which remains to be elucidated. It was observed when enzymatic, spontaneous or chemical hydrolysis of natural or synthetic RNAs was investigated and can be promoted by different factors, including detergents and various proteins (33,34).

Imidazole and spermine–imidazole as structural probes for RNA

A number of small organic molecules capable of cleaving RNA are used as structural probes of RNA (1–6,21,26,36). Several recent studies were directed to the development of new reagents cleaving RNA by *trans*-esterification of the phosphodiester linkages (see e.g. 12 and 13). In this paper we show the potential of imidazole and synthetic constructs with imidazole residues to serve as probes for studying RNA structure in solution. This conclusion is based on the pronounced effect of the $tRNA^{Asp}$ architecture on the hydrolysis of its phosphodiester bonds by these compounds. It is further supported by the structural mapping of an RNA fragment derived from the tRNA-like structure of TMV RNA (Figs 6 and 7). Based on functional and structural properties of viral tRNA-like domains, this molecule should correspond to a histidine accepting minihelix mimicking the amino acid accepting end of a tRNA and should contain a pseudo-knot (Fig. 7). Functional assays have indeed verified the ability of this RNA to be charged by histidine (37). Probing with imidazole and **Sp-Im** indicate cleavages in the four single-stranded regions of the 38 nucleotide-long RNA (Fig. 6). Interestingly, the two connecting single-strands of the 3′-terminal pseudo-knot (L1 and L3 in Figure 7) are well cut, except nucleotide A18 in L1, which was proposed in the case of the satellite virus of TMV (38) to mimic the minus one histidine identity nucleotide present in all canonical $tRNA^{His}$ species. The present chemical data thus support the proposal that this nucleotide is stacked on the acceptor stem over C19 and that its phosphodiester linkage is less flexible to be strongly cut by the imidazole probe. An interesting point concerns the imidazole cleavages observed for the loop between nucleotides U28 and U34, which are consistent with a T-loop conformation found in canonical tRNAs. Indeed, U28 and especially A29 are weakly cut as compared to the other nucleotides of the loop (see Figs 6 and 7 for details), in agreement with a weak flexibility of the phosphodiester bond between C27 and A30 which are geometrically constrained in a T-loop conformation. Indeed, the A30–U34 reverse Hoogsteen pair is stacked on the last base pair of the acceptor branch and the two U28 and U29 nucleotides are stacked one to another in an internal bulge conformation (39).

Conclusions and perspectives

The RNA cleaving compounds investigated in this work represent a new family of tools to study RNA conformation. Hydrolysis in imidazole buffer can be used for easily and readily distinguishing between single-stranded and double-stranded sequences in RNAs. The conjugates with imidazole groups represent simple mimics of RNase A: they contain a structure allowing binding of the molecules to RNA and a residue

catalysing the hydrolysis reaction. These simple molecules have an advantage as structural probes, as compared to RNase A. This cationic enzyme is known to affect RNA structure upon binding and in some cases it easily cleaves RNA at PypPu sequences in double-stranded regions of the molecules. In contrast to the enzyme, the mimics do not unfold RNA structure and they can be expected to cleave only within the true single-stranded sequences of RNA. The developed artificial nucleases might be used for comparison of structures of mutant tRNAs and of other RNA molecules. An interesting feature of the **Sp-Im**/imidazole buffer system is its binary nature. Hydrolysis of RNA by the groups belonging to two different molecules provides a possibility of development of binary RNA cleaving groups which may represent attractive groups for design of second generation antisense oligonucleotide derivatives.

ACKNOWLEDGEMENTS

We thank C. Florentz for advice on RNA cloning and transcription. This work was supported by CNRS, Université Louis Pasteur, International Science Foundation and by Ministry of Science, High Education, and Technical Policy of Russia.

REFERENCES

1 Ehresmann, C., Baudin, F., Mougel, M., Romby, P., Ebel, J.-P. and Ehresmann, B. (1987) *Nucleic Acids Res.*, **15**, 9109–9128.
2 Chow, C.S. and Barton, J.K. (1992) *Methods Enzymol.*, **212**, 219–242.
3 Garcia, A., Giegé, R. and Behr, J.-P. (1990) *Nucleic Acids Res.*, **18**, 89–95.
4 Morrow, J.R., Buttrey, L.A., Shelton, V.M. and Berback, K.A. (1992) *J. Am. Chem. Soc.*, **114**, 1903–1905.
5 Huber, P.W. (1993) *FASEB J.*, **7**, 1367–1374.
6 Pan, T., Dichtl, B. and Uhlenbeck, O.C. (1994) *Biochemistry*, **33**, 9561–9565.
7 Bashkin, J.K., Frolova, E.I. and Sampath, U.S. (1994) *J. Am. Chem. Soc.*, **116**, 5981–5982.
8 Komiyama, M. and Inokawa, T. (1994) *J. Biochem.*, **116**, 719–720.
9 Hall, J., Husken, D., Pieles, U., Moser, H.E. and Haner, R. (1994) *Chem. Biol.*, **1**, 185–190.
10 Magda, D., Miller, R.A., Sessler, J.L. and Iverson, B.L. (1994) *J. Am. Chem. Soc.*, **116**, 7439–7440.
11 Modak, A.S., Gard, J.K., Merriman, M.C., Winkeler, K.A., Bashkin, J.K. and Stern, M.K. (1991) *J. Am. Chem. Soc.*, **113**, 283–291.
12 Tung, C.-H., Wei, Z., Leibowitz, M.J. and Stein, S. (1992) *Proc. Natl. Acad. Sci. USA*, **89**, 7114–7118.
13 Podyminogin, M.A., Vlassov, V.V. and Giegé, R. (1993) *Nucleic Acids Res.*, **21**, 5950–5956.
14 Deakyne, C.A. and Allen, L.C. (1979) *J. Am. Chem. Soc.* **101**, 3951–3959.
15 Breslow, R. (1991) *Acc. Chem. Res.*, **24**, 317–324.
16 Breslow, R. and Labelle, M. (1986) *Am. Chem. Soc.*, **108**, 2655–2659.
17 Breslow, R., Huang, D.-L. and Anslyn, E. (1989) *Proc. Natl. Acad. Sci. USA*, **86**, 1746–1750.
18 Zuber, G., Sirlin, C. and Behr, J.-P. (1993) *J. Am. Chem. Soc.*, **115**, 4939–4940.
19 Wyatt, J.R., Chastain, M. and Puglisi, J.D. (1991) *BioTechniques*, **11**, 764–769.
20 Rether, B., Bonnet, J. and Ebel, J.-P. (1974) *Eur. J. Biochem.*, **50**, 281–288.
21 Romby, P., Moras, D., Bergdoll, M., Dumas, P., Vlassov, V.V., Westhof, E., Ebel, J.-P. and Giegé, R. (1985) *J. Mol. Biol.*, **184**, 455–471.
22 Romby, P., Moras, D., Dumas, P., Ebel, J.-P. and Giegé, R. (1987) *J. Mol. Biol.*, **195**, 193–204.
23 Guilley, H., Jonard, G., Kukla, B. and Richards, K.E. (1979) *Nucleic Acids Res.*, **6**, 1287–1308.
24 Perret, V., Garcia, A., Puglisi, J., Grosjean, H., Ebel, J.-P., Florentz, C. and Giegé, R. (1990) *Biochimie*, **72**, 735–744.
25 Bruce, A.G. and Uhlenbeck, O.C. (1978) *Nucleic Acids Res.*, **4**, 2427–2433.
26 Vlassov, V.V., Giegé, R. and Ebel, J.-P. (1981) *Eur. J. Biochem.*, **119**, 51–59.
27 England, T.E. and Uhlenbeck, O.C. (1978) *Biochemistry*, **17**, 2069–2076.
28 Kirby, A.J. and Marriott, R.E. (1995) *J. Am. Chem. Soc.*, **117**, 833–834.
29 Westhof, E., Dumas, P. and Moras, D. (1983) *J. Biomol. Struc. Dyn.*, **1**, 337–355.
30 Florentz, C., Briand, J.-P., Romby, P., Hirth, L., Ebel, J.-P. and Giegé, R. (1982) *EMBO J.*, **1**, 269–276.
31 Dock-Bregeon, A.-C. and Moras, D. (1987) *Cold Spring Harbor Symp. Quant. Biol.*, **52**, 113–121.
32 Wintermeyer, W. and Zachau, H.G. (1970) *FEBS Lett.*, **11**, 160–164.
33 Kierzek, R. (1992) *Nucleic Acids Res.*, **19**, 5073–5077.
34 Kierzek, R. (1992) *Nucleic Acids Res.*, **19**, 5079–5084.
35 Hosaka, H., Sakabe, I., Sakamoto, K., Yokoyama, S. and Takaku, H (1994) *J. Biol. Chem.*, **269**, 20090–20094.
36 Krzyzosiak, W.J., Marciniec, T., Wiewiorowsky, M., Romby, P., Ebel, J.-P. and Giegé, R. (1988) *Biochemistry*, **27**, 5771–5777.
37 Felden, B. (1994) Thèse de l'Université Louis Pasteur de Strasbourg.
38 Felden., B., Florentz, C., McPherson, A., Giegé, R. (1994) *Nucleic Acids Res.*, **22**, 2882–2886.
39 Rich, A. and RajBhandary, U.L. (1976) *Annu. Rev. Biochem.*, **45**, 805–860.
40 Gangloff, J., Keith, G., Ebel, J.-P. and Dirheimer, G. (1971) *Nature NB*, **230**, 125–127.
41 Westhof, E. and Jaeger, L. (1992) *Curr. Opin. Struct. Biol.*, **2**, 327–333.